JOINT INVERSION OF CSAMT-LOTEM DATA FROM MERAPI

Supriadi, R*., Hördt, A.**, Müller, M.**, Hanstein, T.**

*)Physics Department, UNNES Semarang, and Earth Physics Laboratory, ITB Bandung, Indonesia
Jl. Raya Sekaran, Gunung Pati Semarang, ph. +62 024 7475650, e-mail :
mipaunes@smg.mega.net.id ; supriadi@fisbum.fi.itb.ac.id

**) Institut für Geophysik und Meteorologie, Universität zu Köln, Albertus Magnus Platz, 50923 Köln

Abstract

One-dimensional CSAMT and CSAMT-LOTEM joint inversion are implemented into an existing 1-D joint inversion code. Instead of apparent resistivity and phase impedance, real and imaginary parts of the impedance are used as inverted data to avoid artificial data in near-field region and unsymmetrical scale between the two types of data. Since the values of the imaginary component can be negative, the inverse hyperbolises function is used to represent the logarithmic feature of the data. By testing to the synthetic data, the use of real and imaginary component of the impedance as inversion variables give relatively the same quality in estimating inverted model, but with less iteration number. The inversion routine is also successfully applied to the CSAMT and LOTEM data at Merapi both as singles and joint inversion .

1. Introduction

Due to very high resistivity contrast on volcanoes, electromagnetic methods are strongly recommended both for structural and monitoring purposes (Lenat, 1995). The resistivity measurements at Merapi have been done by several researchers with different techniques, i.e. : MT by Hoffmann-Rothe et al.(1998), LOTEM by Müller et al. (1998) and dc geoelectrics by Friedel et al. (1998). Parallel to the LOTEM survey and using the same transmitter, a CSAMT survey was carried out at the same locations (Supriadi et al., 1999).

The CSAMT-LOTEM joint measurement at the same stations provides an opportunity to do joint interpretation in order to reduce the ambiguity inherent in the individual methods. Vozoff and Jupp (1975) showed the advantages of jointly inverting the MT and Schlumberger sounding data sets to resolve a thin resistive layer not seen by either the MT or dc methods. Other examples of joint inversion were presented by Raiche et al (1985) for coincident loop transient EM with Schlumberger sounding, and by Hördt (1989) for MT with LOTEM.

Goldstein and Strangway (1975) introduced the use of Controlled Source Audio Magnetotelluric (CSAMT) to overcome the signal strength and unreliable source orientation problems that arise in magnetotelluric (MT) method. However, the non plane wave nature of the source limits the interpretation of data by conventional MT methods. For this reason, Routh and Oldenburg (1999) developed a technique for inverting complete CSAMT data sets without any correction.

The data to be inverted in either MT or CSAMT usually are apparent resistivity and phases which are not the original data recorded in those systems, rather these data are derived from the impedance tensor using plane-wave formulation. In near-field region of CSAMT data, the Cagniard apparent resistivity lost its conceptual meaning since the plane-wave assumption in that region is no longer

valid. Recognizing this, we develop a CSAMT inversion based on the original source-free data, the impedance of the medium i. e : the real and imaginary parts of the impedance tensor. Since the real and imaginary parts can become negative and have large dynamic range, instead of normal logarithmic transformation, inverse hyperbolicus function is implemented.

The paper starts with formulations of real and imaginary parts of the impedance along with its inverse hyperbolicus transformation in CSAMT inversion. Next, we test our inversion with synthetic data. We then apply the inversion to CSAMT data at Merapi either as a single or joint inversion with LOTEM.

2. CSAMT Inversion

In controlled-source magnetotellurics, the data (coming into the receiver) are complex orthogonal electric (E) and magnetic (H) fields. Using electric dipole and magnetic coil as sensors for E and H fields respectively, the magnitudes of E and corresponding perpendicular H fields are measured. Unlike in MT, the absolute phases of each electric and magnetic fields namely Φ_E and Φ_H are also recorded in CSAMT system by synchronizing the receiver and transmitter clocks before measuring. Inverting the original data deals with four data sets namely Ex, Hy, Φ_{Ex} and Φ_{Hy} for X-Y polarization or Ey, Hx, Φ_{Ey} and Φ_{Hx} for Y-X polarization, and needs accurate information on source current. This may not practical.

As in MT, the existing CSAMT inversion uses apparent resistivity and phase impedance as inverted data (Routh and Oldenburg, 1999). The original CSAMT data are scaled by the frequency (f) to get plane-wave apparent resistivity (ρ_a) as

$$\rho_a = \frac{1}{5f}\left|\frac{E}{H}\right|_{\perp}^2 \qquad \ldots(1)$$

where the symbol $\perp$ denotes any perpendicular pairs of E and H fields, while from Φ_E and Φ_H, the phase impedance (PHI_a) is easilly determined as

$$PHI_a = \Phi_E - \Phi_H \qquad \ldots(2)$$

In CSAMT, due to the presence of the source, the apparent resistivity in near-filed region does not depend on frequency, instead, it depends on the transmitter-receiver separation as in dc method (Zonge and Hughes, 1991). Equation (1) therefore does not apply for the whole CSAMT data range, i.e, it may apply for far-field but not for near-field data. We suggest to invert the real and imaginary parts of the complex impedance Z according to the relation:

$$\mathbf{Z} = \frac{\mathbf{E}}{\mathbf{H}} \qquad \ldots(3)$$

where **E** and **H** are orthogonal complex electric and magnetic fields. Unlike apparent resistivity and phase impedance, the real and imaginary parts of the impedance are source-free and reflect the original data coming to the CSAMT receiver which are valid for complete CSAMT data range. They also have the same scale and range that makes possible to use the same weighting in the inversion routine.

In addition to the earth's model parameters (resistivity and thickness of the layers) as in other EM methods, the CSAMT forward modelling needs source and receiver parameters namely receiver positions (Rx and Ry) relative to the centre of

the transmitter. Unlike apparent resistivity which always has positive values, real and imaginary parts of the impedance for certain model can become negative. Figure 1 shows examples of calculated real and imaginary parts of the impedance in Ω as a function of frequency for three-layer earth model with resistivities of 1000 Ωm for the top, 30 Ωm for the second and 2000 Ωm for the basement layer, and thickness of 400 m for each layers. The receiver is located at position Rx=12000 m and Ry= 1200 m relative to the center of the x-directed transmitter. As shown in figure 1, the real and imaginary parts of the impedance almost have the same range of data up to 6 Ω, except in frequencies equal to and lower than 2 Hz where the imaginary part has negative values.

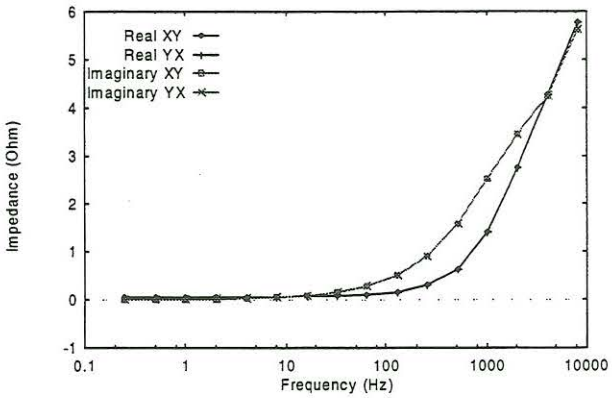

Figure 1. Real and imaginary parts of the impedance of YX polarization as a function of frequencies for for three-layer earth model with resistivities of 1000 Ωm for the top , 30 Ωm for the second and 2000 Ωm for the basement layer, and thickness of 400 m for each layers. The receiver is located at position Rx=12000 m and Ry= 1200 m relative to the center of the x-directed transmitter

Since geophysical properties such as resistivities and depths can vary over several orders of magnitude and must be positive, it is desirable to invert for the logarithms of the parameters. The use of logarithmic parameters makes the Jacobian have more stable inverse, i.e the sums of squares of the elements of the columns are of the same order of magnitude. Logarithmic data representation is also desired in order not to distinguish between error in the predicted data and error in the observed data. The use of logarithmic data also tends to improve the condition of the influence matrix, i.e the sums of squares of the elements in different rows are of the same order of magnitude.

In order to get the logarithmic values of the two positive and negative data, both field and synthetic data sets are transformed into new data sets using inverse hyperbolicus function as:

$$Y = \ln \frac{1}{a}\left(x + \sqrt{\left(x^2 + a^2\right)}\right) \qquad \ldots(4)$$

where x and y are the old and new data respectively, and **a** is the scaling factor which reflects the transition between linear and logarithmic distribution of the data. For x much smaller than **a**, the data is treated linear, while for x much greater than **a**, the data is logarithmic.

3. Test of CSAMT inversion using synthetic data

Two sets of synthetic data of broad-side and collinear configuration are used to test the CSAMT inversion routine, where the latter contains negative values. Figure 2 shows the comparison between synthetic and inverted data for each real and imaginary components of the two configurations. The inverted data was calculated for the optimum values of the scaling factor **a** that gives the best model misfit and reasonable data misfit. Since it depends on the range and distribution of the observed data, the value of **a** must be determined prior to the iteration.

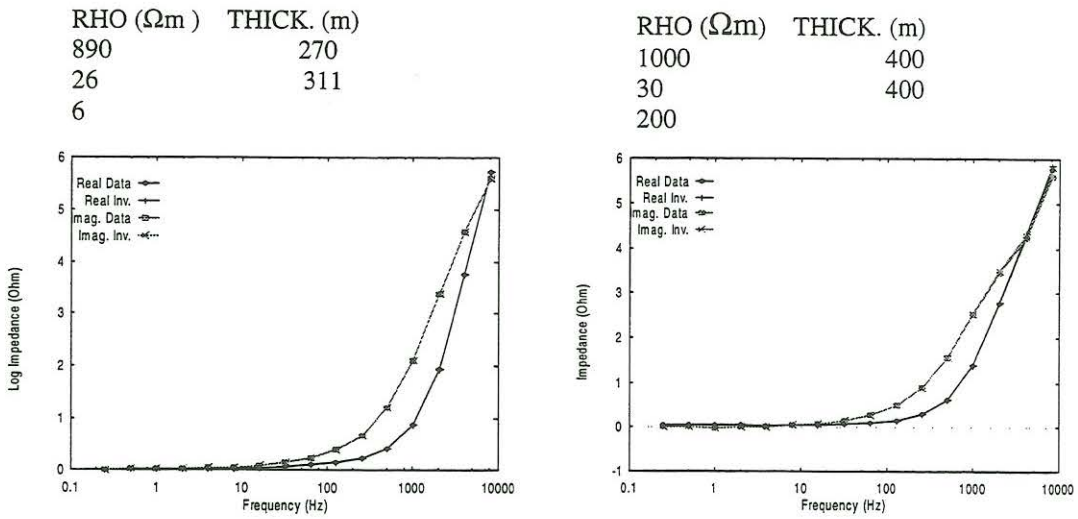

Figure 2. Comparison between synthetic and inverted data of real (dots and lines) and imaginary (rectangles and crosses) parts of the impedance for broad-side (left) and collinear (right) configuration. For the broadside case, the receiver is placed at position of (Rx, Ry) = (279, 2863.9) m relative to the center of the transmitter which has a dipole length of 826,6 m and electrical current of 6 A. For collinear configuration, the receiver is located at (Rx, Ry) = (12000, 1200) m with transmitter current of 10 A and dipole length of 1000 m. The values above each figure are the corresponding parameters of true models.

The value of **a** is critical since it significantly influence the speed of convergence and the model misfit. In general, the number of iterations decreases as **a** increases. By experiment, the optimum scaling factor satisfying :

$$a_{opt} = \frac{X_{max}}{10.n} \qquad \ldots(5)$$

gives the best estimation to the inverted model, where X_{max} and n are the maximum data value and the number of orders of magnitudes of the data, respectively. The choice of scaling factor **a** less than a_{opt} also produces relatively good inverted model but with lower speed of convergence. At **a** larger than a_{opt}, the inverted model starts to deviate from the true model. More detail explanation about the effects of **a** on the speed of convergence, data and model misfit can be found in table 1.

Table 1 illustrates the effects of the scaling factor (a) in the inversion parameters, namely the number of iteration (I), data and model misfit for three-layer earth model in a broad-side configuration (see figure 2). As shown in row 1, as a increases the number of iteration (I) decrease and as a equal to 0.001 that is

the smallest value of the data (column 4), the convergence is still faster (I =7) than that for normal logarithmic representation indicated by I = 9 (column 9).

In column 6, the value of a equal to a_{opt} = 0.143 gives the best data and model misfit, however the values of a less than a_{opt} (column 4 and 5) also give a relatively good prediction to the inverted model with slightly increasing data misfit. Eventhough they give a reasonable data misfit for a > a_{opt} (column 7 and 8), the inverted models start to deviate significantly from the true model, for example as a = 1.0, the inverted resistivity of the basement is 7.75 Ωm compared to 6 Ωm of the true model, and the thickness of the second layer is 293 m compared to 311 m of the true model. Larger model misfit is observed for a = 5.0 where the inverted resistivity of the basement is 9.63 Ωm and the thickness of the second layer is 333.95 m. Compared to the logarithmic counterpart, as long as a less than or equal to a_{opt} , the use of the inverse hyperbolicus function produces relatively the same quality in predicting the earth's model, but with better speed of convergence.

Table 1. The effects of the scaling factor in the inversion parameters. Column 2 and 3 are the true synthetic and initial model respectively, column 4 through 8 are the inverted models for various values of **a**, and column 9 is the inverted model for the normal logarithmic representation.

Scaling faktor (a)			0.001	0.01,	**0.143 =Xmax./10.n**	1.0	5.0	Logarithmic
Iteration number (I)			7	6	4	4	3	9
Data rms (%)			0.4220	0.1645	0.0312	0.1117	0.0905	0.1211
Parameter	True	Initial	Inverted	Inverted	Inverted	Inverted	Inverted	Inverted
RHO1 (Ωm)	**890**	1000	*885.25*	*888.94*	**890.04**	890.25	890.23	887.95
RHO2 (Ωm)	**26**	100	26.07	26.04	**26.03**	26.20	*27.88*	26.03
RHO3 (Ωm)	**6**	10	6.09	6.05	**6.06**	*7.75*	*9.63*	6.04
THICK.1 (m)	**270**	500	269.74	269.92	**269.99**	270.08	268.65	269.89
THICK.2 (m)	**311**	500	310.10	310.68	**311.01**	*293*	*333.95*	310.62

4.The CSAMT and CSAMT-LOTEM joint Inversion of the Merapi data

The CSAMT survey at Merapi was carried out during 8 weeks in the middle of 1998 by Earth's Physics Laboratory, ITB, using the Zonge electromagnetic equipment set. In parallel, a LOTEM survey was also carried out by IGM University of Cologne, Germany at ten stations where 6 of them took place at the same locations as the CSAMT's including the highest station at Pasar Bubar. Distribution of stations, transmitter locations and the presentation of data can be found in Supriadi et al.(1999) for CSAMT and Müller et al. (1998) for LOTEM.

The real and imaginary data at station K23XY98 are inverted. The comparison between observed and calculated CSAMT along with its final model is shown in figure 4. The data is well explained by a one-dimensional two-layer earth with top resistivity of 68 Ωm and basement of 5 Ωm at the depth of 300 m.

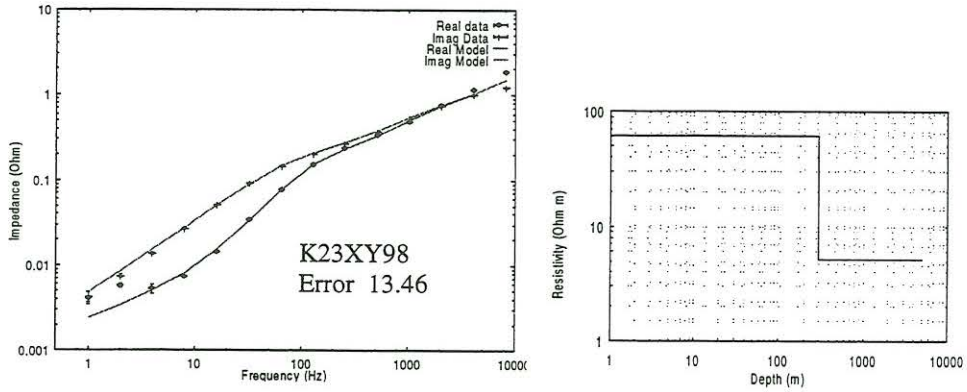

Figure 3. Examples of fitting (left) between the single CSAMT inverted (lines) and observed real and imaginary component of the impedance at station K23XY98 along with its final model (right)

Besides the single CSAMT inversion, the CSAMT-LOTEM joint inversion was also sucessfully implemented in an existing 1-D joint inversion code for LOTEM and MT data (Hördt, 1989). The XY polarization of the CSAMT and vertical magnetic component of the LOTEM data at station Pasar Bubar are jointly inverted to test the routine. Figure 4 shows comparison between the single CSAMT-LOTEM inverted data with its joint counterpart. As shown in figure 4, data misfit is 1.9 % for the single CSAMT and 15,5 % for the single LOTEM, and 16,67 % for the CSAMT-LOTEM joint inversion. A better fit is obtained with the individual inversion.

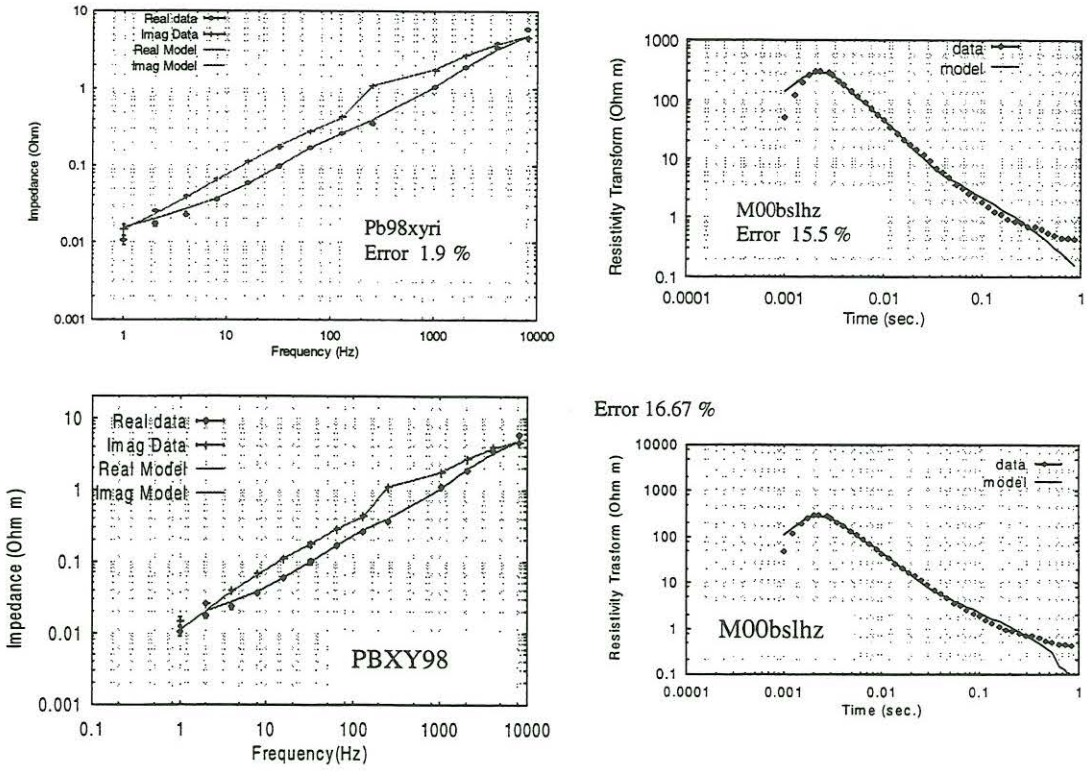

Figure 4. Comparison between individual with joint CSAMT- LOTEM inverted data at Station Pasar Bubar. Top : matching of the single CSAMT real and imaginary parts of the impedance (left) and of the single vertical magnetic LOTEM apparent resistivity (right), bottom : matching of the CSAMT-LOTEM joint inversion.

Figure 5 compares the individual with joint CSAMT and LOTEM inverted model. As shown in figure 5, the final model of the joint inversion coincides with that of the single CSAMT inversion at shallower region and with that of the single LOTEM inversion at deeper structure. It may mean that, if the joint model is more realistic than the individual model, CSAMT and LOTEM complement each other in depth investigation range where CSAMT has depth resolution better than LOTEM at shallower structure, while LOTEM has better resolution at deeper region.

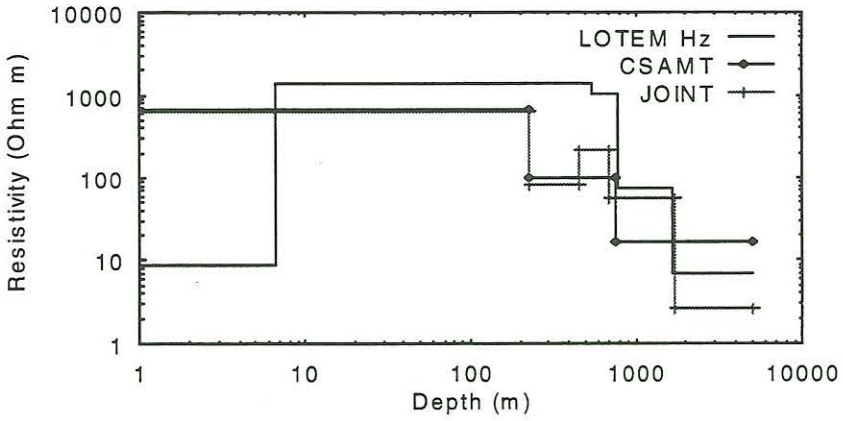

Figure 5. Comparison between individual with joint CSAMT and LOTEM inverted model for Station Pasar Bubar.

5.Concluding Remarks

By testing both synthetic and Merapi data, the CSAMT and CSAMT-LOTEM joint inversions are successfully implemented into an existing code for LOTEM and MT joint inversion. Rather than apparent resistivity and phase impedance, the use of real and imaginary component of the impedance as inverted data in the CSAMT inversion has some advantages, i.e 1). It avoids dealing with artificial data especially in near-field region, and 2) rather than normal logarithmic representation, the use of the inverse hyperbolicus transformation increases the speed of convergence and makes possible to handle negative data. For the station Pasar Bubar (Pbxy98 for CSAMT or M00bslhz for LOTEM), the CSAMT-LOTEM joint inverted model coincides with the CSAMT's at shallower region and relatively close to the LOTEM's at deeper structure. The slight different of data misfit between the singles and joint inversions indicates one-dimensionality of the structure at that station.

6. Acknowledgements

This work is part of research collaboration between Earth's Physics Laboratory, ITB, Indonesia and IGM University of Cologne, Germany. The author thanks the DLR Germany for the sponsorship during his 4-months stay in Cologne. He thanks also Earth's Physics Laboratory , ITB for part of the flight ticket expenses.

7. References

Friedel, S., F. Jacobs, Ch. Flechsig, C. Reismann, and I. Bruner, **Large-scale DC Resistivity Imaging at Merapi volcano**, in Decade volcanoes Under Investigation, Editors : J. Zchau and M. Westerhaus, Bd. III/1998, 47-52, *Dt. Geophys. Gesellschaft*, 1998.

Goldstein, M., A., and D., W. Strangway, 1975, **Audio frequency magnetotellurics with a grounded electric dipole source**, *Geophysics, vol.40, p.669-683.*

Hördt, A., 1989, Ein Verfahren zur "Joint Inversion" angewandt auf "Long Offset Transient Electromagnetics" (LOTEM) und "Magnetotelurik" (MT) Diplom thesis-geophysics, University of Cologne, (unpublished).

Hoffman-Rothe, A., A. Müller, O. Ritter, and V. Haak , **Magnetotelluric Survey at merapi Volcano and across Java, Indonesia**, in Decade volcanoes Under Investigation, Editors : J. Zchau and M. Westerhaus, Bd. III/1998, 47-52, *Dt. Geophys. Gesellschaft*, 1998.

Lenat, J., F., 1995, **Geoelectrical methods in volcano monitoring, in Monitoring active volcanoes**, by McGuire, B., Kilburn, C. and J. Murray, 248-274, *UCL Press.*

Müller, M., Hördt, A., and Neubauer, F., A., 1998, **A LOTEM survey on Mt. Merapi 1998, in Decade volcanoes Under Investigation**, Editors : J. Zchau and M. Westerhaus, Bd. III/1998, 41-46, *Dt. Geophys. Gesellschaft*, 1998.

Raiche, A. P., Jupp, D. L. B., Rutter, H. and K. Vozoff, 1985, **The joint use of coincident loop transient electromagnetic and Schlumberger sounding to resolve layered structures**, *Geophysics, 50, 1618-1627*

Routh, P., S., and D., W., Oldenburg, 1999, **Inversion of controlled-source audio frequency magnetotellurics data for a horizontaly layered earth**, *Geophysics, vol 64, no. 6, p. 1689-1697.*

Supriadi, D. Sutarno, A. Singarimbun, L. Hendrajaya and D. Santoso, 1999, **Structural investigation of Merapi volcano using Controlled-source audio magnetotellurics (CSAMT)**, *Proceeding, Association of Indonesian Geophysicists (PIT HAGI) XXIV*, Surabaya.

Vozoff, K., Jupp, D. L. B., 1975, **Joint Inverion of Geophysical Data**, *Geophys. J. Roy. Astr. Soc., 42, 977-991.*

Zonge, K., L., and L., J., Hughes, 1991, **Controlled-Source Audio Frequency Magnetotellurics**, *in Nabighian, M., N., Ed., Electromagnetic Methods in Applied Geophysics-Theory*, Volume II : Soc. Expl. Geophys., 713-809.